



1 **Mediterranean nascent sea spray organic aerosol and** 2 **relationships with seawater biogeochemistry**

3 Evelyn Freney¹, Karine Sellegri¹, Alessia Nicosia¹, Jonathan T. Trueblood¹, Matteo. Rinaldi³,
4 Leah. R. Williams⁴, André. S. H. Prévôt⁵, Melilotus Thyssen⁶, Gérald Grégori⁶, Nils
5 Haëntjens⁷, Julie Dinasquet^{8,9*}, Ingrid Obernosterer⁹, France Van-Wambeke⁶, Anja Engel¹⁰,
6 Birthe Zäncker¹⁰, Karine Desboeufs¹¹, Eija Asmi², Hilka Timmonen², Cécile Guieu¹²

7 ¹ Université Clermont Auvergne, CNRS, Laboratoire de Météorologie Physique (LaMP) F-63000 Clermont-
8 Ferrand, France

9 ² Atmospheric Composition Research, Finnish Meteorological Institute, Helsinki, FI-00101, Finland

10 ³ National Research Council (CNR), Institute of Atmospheric Sciences and Climate (ISAC), Bologna, Italy

11 ⁴ Aerodyne Research, Inc., Billerica, Massachusetts, USA

12 ⁵ Laboratory of Atmospheric Chemistry, Paul Scherrer Institute, 5232 Villigen PSI, Switzerland

13 ⁶ Aix-Marseille University, Toulon University, CNRS, IRD, Mediterranean Institute of Oceanography UM110,
14 Marseille 13288, France

15 ⁷ School of Marine Sciences, University of Maine, Orono, ME 04469, USA

16 ⁸ Marine Biology Research Division, Scripps Institution of Oceanography, 92037 La Jolla, US

17 ⁹ CNRS, Sorbonne Université, Laboratoire d'Océanographie Microbienne, UMR7621, F-66650 Banyuls-sur-
18 Mer, France

19 ¹⁰ GEOMAR, Helmholtz Centre for Ocean Research Kiel, 24105 Kiel, Germany

20 ¹¹ LISA, CNRS UMR7583, Université Paris Est Créteil (UPEC), Université de Paris, Institut Pierre Simon
21 Laplace (IPSL), Créteil, France

22 ¹² Sorbonne Université, CNRS, Laboratoire d'Océanographie de Villefranche, LOV, F-06230 Villefranche-sur-
23 Mer, France

24

25 * now at Center for Aerosol Impacts on Chemistry of the Environment, CASPO, Scripps Institution of
26 Oceanography, UCSD, USA

27 *Correspondence to:* evelyn.freney@uca.fr

28 **Abstract**

29 The organic mass fraction from sea spray aerosol (SSA) is currently a subject of intense research. The majority
30 of this research is dedicated to measurements in ambient air, although recently a small number of studies have
31 additionally focused on nascent sea spray aerosol. This work presents measurements collected during a five-
32 week cruise in May and June, 2017 in the central and western Mediterranean Sea, an oligotrophic marine region
33 with low phytoplankton biomass. Surface seawater was continuously pumped into a bubble bursting apparatus to
34 generate nascent sea spray aerosol. Size distributions were measured with a differential mobility particle sizer
35 (DMPS). Chemical characterization of the submicron aerosol was performed with a time of flight aerosol
36 chemical speciation monitor (ToF-ACSM) operating with a 15-minute time resolution, and with filter-based
37 chemical analysis on a daily basis. Using a positive matrix factorization analysis, the ToF-ACSM non-refractory
38 organic matter (OM_{NR}) was separated into four different organic aerosols types which were identified as primary



39 OA (POA_{NR}), oxidized OA (OOA_{NR}), a methanesulfonic acid type OA ($\text{MSA-OA}_{\text{NR}}$) and a mixed OA (MOA_{NR}).
40 In parallel, surface seawater biogeochemical properties were monitored providing information on phytoplankton
41 cell abundance and seawater particulate organic carbon (one-hour time resolution), and seawater surface
42 microlayer (SML) dissolved organic carbon (DOC) (on a daily basis). Statistically robust correlations (for
43 $n > 500$) were found between MOA_{NR} and nano phytoplankton cell abundance, as well as between POA_{NR} ,
44 OOA_{NR} and particulate organic carbon (POC). Filter-based analysis of the submicron SSA showed that the non-
45 refractory organic mass represented only $13 \pm 3\%$ of the total organic mass, which represents $22 \pm 6\%$ of the total
46 sea spray mass. Parameterizations of the contributions of different types of organics to the submicron nascent sea
47 spray aerosol, are proposed as a function of the seawater biogeochemical properties for use in models.

48 **1 Introduction**

49 Oceans cover approximately 70% of the Earth's surface and sea spray emissions contribute up to 6 kTons/Yr of
50 particulate matter, making them a major primary source in the atmosphere. The majority of the mass associated
51 with sea spray emissions is in the form of coarse mode sea salt particles. However, it is now well known that the
52 submicron fraction of marine emissions is also important and contains a significant portion of organic
53 compounds (Facchini et al., 2008). This organic fraction tends to be highest during phytoplankton bloom events
54 (O'Dowd et al., 2004). Although the organic fraction of the aerosol population represents little mass, the high
55 number concentration of these aerosol particles makes them a significant contributor to the potential cloud
56 condensation nuclei concentration (Burrow et al. 2018). Organics in sea spray have also been shown to
57 contribute to potential marine ice nuclei (McCluskey et al., 2017). Understanding how the organic fraction of
58 marine aerosol particles transfer to the atmosphere is essential to help identify the contribution of the marine
59 aerosols to the Earth's radiative budget.

60 In general, sea spray aerosol is generated through bubble bursting after wave breaking at the ocean surface, a
61 process that has been described in early publications (Blanchard and Woodcock, 1980). Once bubbles burst, film
62 and jet droplets are ejected into the atmosphere, and dry to leave aerosol particles as residues containing the
63 different constituents of the bulk seawater and surface microlayer. The size distribution of this sea spray extends
64 from the fine particle range, with diameters < 100 nm to the super-micron range (up to $3 \mu\text{m}$). The super-micron
65 range is known to be mainly composed of refractory NaCl and different MgCO_3 or $(\text{Mg})_2\text{SO}_4$ species, while the
66 submicron fraction tends to be enriched with organic compounds (O'Dowd et al., 2004).

67 Traditionally, measurements in and around the marine boundary layer were made using offline filter
68 measurements followed by laboratory-based analysis using either ion chromatography or organic carbon and
69 elemental carbon analysis. However, over the last decade, there has been a significant increase in the number of
70 studies deploying online aerosol mass spectrometry methods, including laser ablation mass spectrometry
71 (Dall'Osto et al., 2019) and thermal vaporization followed by electron impact ionization methods (Giordano et
72 al., 2017; Ovadnevaite et al., 2011; Schmale et al., 2013).

73 The aerosol mass spectrometer (AMS, Aerodyne Research, Inc) and aerosol chemical speciation monitor
74 (ACSM) are examples of the latter type and are widely used instruments to monitor the chemical composition of
75 submicron particulate matter in the atmosphere. The design of this instrument is optimized to investigate the
76 non-refractory fraction, defined as material that vaporizes at 600°C of aerosol mass in the atmosphere. In the



77 majority of atmospheric environments, the submicron fraction of the aerosol is dominated by non-refractory
78 organic and inorganic species. In marine environments, the AMS has also been shown to be a useful tool in
79 characterizing submicron sea-salt aerosols (Ovadnevaite et al., 2011) and even more so organic aerosols related
80 to marine emissions.

81 Aerosol mass spectrometry has been used recently to better characterize the chemical properties of ambient
82 marine aerosol particles, from the Atlantic (Ovadnevaite et al., 2011), to Antarctic (Schmale et al., 2013,
83 Giordano et al., 2017) coastal environments. Using a combination of high-resolution aerosol mass spectrometry
84 and positive matrix factorization analysis, different marine organic aerosols have been identified including
85 secondary marine organic aerosols, methanesulfonic acid (MSA), containing organic aerosols, and amino acid
86 (AA) associated organic aerosols thought to be primarily linked to local sea life emissions at the measurement
87 site.

88 Most of these studies measured ambient aerosol already modified through atmospheric chemical and physical
89 processes. Current knowledge on the source and evolution of nascent sea spray organic emissions is still limited.
90 This is attributed to the natural variability of marine organic aerosol and to the lack of high temporal resolution
91 studies at the ocean/atmospheric interface. A very limited number of studies have focused directly on the
92 composition of nascent sea spray aerosol particles emitted from wave action in controlled simulation chambers
93 (Wang et al., 2015) or through dedicated bubble bursting experiments (Bates et al., 2012; Dall'Osto et al., 2019).
94 These studies in controlled environments identified the presence of aliphatic-rich and amino acid-rich organic
95 aerosols related to different phases of phytoplankton blooms (Bates et al. 2012; Wang et al., 2015). Dall'Osto et
96 al., (2019) identified an amino acid contribution in both nascent sea spray aerosol and ambient aerosols.

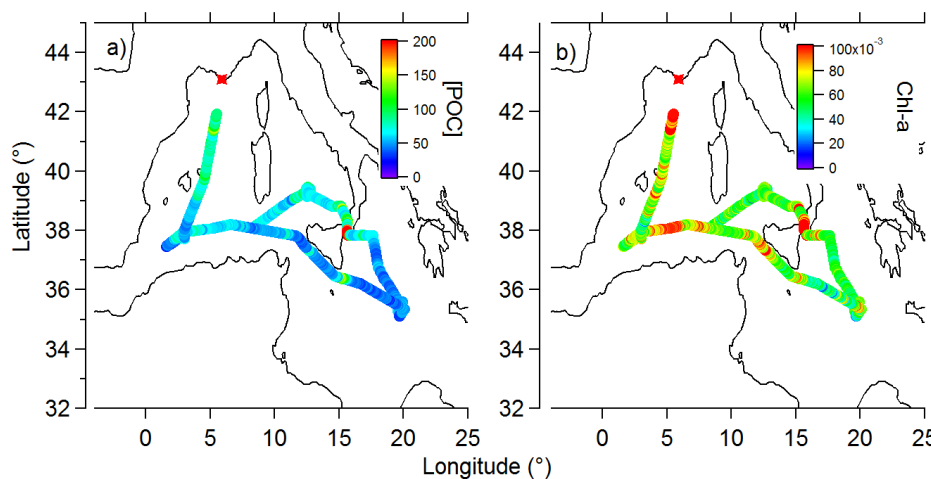
97 In this work, we characterized nascent sea spray submicron aerosol generated from the underway seawater
98 system of the R/V *Pourquoi Pas?* over a five-week campaign in the Mediterranean Sea. The Mediterranean Sea
99 is a low nutrient low chlorophyll (LNLC) environment and was characterized by oligotrophic conditions along
100 the whole field campaign (Guieu et al., 2020). Understanding the formation of nascent sea spray aerosols in such
101 an LNLC system can provide valuable information and be extrapolated to other oligotrophic environments.

102 **2-Methodology**

103 **2.1 The PEACETIME oceanographic campaign**

104 The French research vessel, the R/V *'Pourquoi Pas?'*, was deployed for a five-week-long period from the 10th of
105 May to the 10th of June 2017 on the Mediterranean Sea, as part of the project: PEACETIME (ProcEss studies at
106 the Air-sEa Interface after dust deposition in The Mediterranean sea) project. The ship track (Fig. 1) started and
107 ended in La Seyne sur Mer, France. The ship traveled clockwise covering latitudes in the Mediterranean Sea
108 from 35° to 42°, and longitudes from 0° to 21°.

109 La Seyne s/Mer, France.



110

111 **Figure 1: The ship track in the Mediterranean Sea during the PEACETIME expedition. The**
112 **trajectory is colored by a) POC b) *Chl-a*. . The red star indicates the location of the starting**
113 **point La Seyne sur Mer.**

114 Results from a suite of hydrology and biogeochemistry measurements performed on board are given in Guieu et
115 al. (2020). In addition to standard seawater temperature (T) and salinity (S) measurements, the concentrations of
116 a wide range of chemical and microbiological parameters were monitored hourly. Several plankton functional
117 groups were identified, including *Synechococcus*, *Prochlorococcus*, nanoeukaryotes, *Coccolithophores*-like,
118 *Cryptophytes*-like, and microphytoplankton. The sea surface temperature (T) showed a gradual increase from
119 the start to the end of the campaign from 19°C up to 23°C. Sea surface salinity (S) varied from 36 up to 39 g l⁻¹
120 increasing from east to west. The sampling region was characteristic of open sea (average depth 2750 m ± 770 m
121 along the transect). The sea was calm to moderately rough throughout the sampling period with conditions
122 always remaining below Beaufort 4. Wind speed varied between 10 and 20 m s⁻¹.

123 Total chlorophyll-a (*Chl-a*) and particulate organic carbon (POC) were also measured. In line with the
124 oligotrophic state of the Mediterranean Sea during this period. POC concentrations were highest at the most
125 northern longitudes and gradually decreased along the ship transect (Fig. 1a), the *Chl-a* concentration remained
126 stable and low (0.07 ± 0.03 mg m⁻³) throughout the sampling period (Fig. 1b).

127 2.2. Surface Seawater Analysis

128 2.2.1. Flow cytometry

129 Phytoplankton cells were counted with one-hour time resolution using an automated Cytosense flow cytometer
130 (Cytobuoy, NL), connected to a continuous clean pumping underway seawater system, as described in Thyssen
131 et al. (2010) and Leroux et al. (2017). Particles were brought within a laminar flow filtered seawater sheath fluid,
132 and detected with forward scatter (FWS) and sideward scatter (SWS) as well a fluorescence in the red (FLR
133 >652 nm) and orange (FLO 552-652 nm) in the size range 1- 800 μm. Two trigger levels were applied for the
134 distinction between highly concentrated picophytoplankton and cyanobacteria groups (trigger level FLR 7.34



135 mV, sampling at a speed of $4 \text{ mm}^3 \cdot \text{s}^{-1}$ and analyzing $0.65 \pm 0.18 \text{ cm}^3$, and lower concentrated nano- and micro
136 phytoplankton (trigger level FLR 14.87 mV, at a speed of $8 \text{ mm}^3 \cdot \text{s}^{-1}$ and analyzing $3.57 \pm 0.97 \text{ cm}^3$). Different
137 sets of 2D projections were plotted in Cytocclus® software to manually gate phytoplankton groups. To follow
138 stability of the flow cytometer, $2 \mu\text{m}$ red fluorescing polystyrene beads (Polyscience) were regularly analyzed.
139 The use of silica beads (1, 2, 3, 5, $7 \mu\text{m}$ in diameter, Bangs Laboratory) for size retrieving estimates from FWS
140 were used to separate picoplankton from nanoplankton clusters.

141 2.2.2. Chlorophyll-a and POC

142 From the underway seawater system, *Chl-a* was derived from the particulate absorption spectrum line-height at
143 676 nm (Bloss et al., 2013) after the relationship was adjusted to PEACETIME *Chl-a* derived from HPLC (*Chl-a*
144 $= 194.41 \times \text{line_height}^{1.131}$). POC was estimated from particulate attenuation at 660 nm using an empirical
145 relationship specific to PEACETIME ($\text{POC} = 1405.1 \times c_p(660) - 52.4$) slightly higher than the literature value
146 which is likely due to the small dynamic range (1.27 higher on average for the range observed (Cetinic et al.,
147 2012)). Both particulate attenuation and absorption of surface water were measured continuously with a
148 WetLabs Spectral Absorption and Attenuation Meter using a flow-through system similar to the setup described
149 in Slade et al. (2010).

150 2.2.3. Heterotrophic bacteria counts and bacterial production

151 For the enumeration of heterotrophic bacteria of discrete samples collected using the Niskin surface bottle
152 ($<5\text{m}$), subsamples (4.5mL) were fixed with glutaraldehyde grade I 25% (1% final concentration), and incubated
153 for 30 min at $4 \text{ }^\circ\text{C}$, then quick-frozen in liquid nitrogen and stored at $-80 \text{ }^\circ\text{C}$ until analysis. Samples were thawed
154 at room temperature. Counts were performed on a FACSCanto II flow cytometer (Becton Dickinson) equipped
155 with 3 air-cooled lasers: red (633 nm), blue (488 nm), red (633 nm) and violet (407 nm). For the enumeration of
156 heterotrophic bacteria, cells were stained with SYBR Green I (Invitrogen – Molecular Probes) at 0.025% (vol /
157 vol) final concentration for 15 min at room temperature in the dark. Stained cells were discriminated and
158 enumerated according to their right-angle light scatter (SSC) and green fluorescence using a $530/30 \text{ nm}$ bandpass
159 filter. In a plot of green versus red fluorescence, heterotrophic bacteria were distinguished from autotrophic
160 prokaryotes. Fluorescent beads ($1.002 \mu\text{m}$; Polysciences Europe) were systematically added to each analyzed
161 sample as an internal standard. The cell abundance was determined from the flow rate, which was calculated
162 with TruCount beads (BD biosciences).

163 Heterotrophic prokaryotic production (BP) was estimated from rates of 3H leucine incorporation using the micro
164 centrifugation technique. The detailed protocol is available in Van wambeke et al (this issue). Briefly, triplicate
165 1.5 mL subsamples from the Niskin surface bottle ($<5\text{m}$) and one blank were incubated in the dark at in situ
166 temperature. Leucine was added at 20 nM final concentration and the leucine - carbon conversion factor used
167 was 1.5 kgC mol^{-1}

168 2.3. Surface MicroLayer (SML) Sampling and Analysis

169 2.3.1. Sampling

170 Surface microlayer SML sampling was conducted from a zodiac using a $50 \times 26 \text{ cm}$ silicate glass plate sampler
171 (Harvey 1966; Cunliffe and Wurl 2014) with an effective sampling surface area of 2600 cm^2 considering both
172 sides. For sampling, the zodiac was positioned 0.5 nautical miles away from the research vessel and into the



173 wind direction to avoid contamination. The glass plate was immersed perpendicular to the sea surface and
174 withdrawn at $\sim 17 \text{ cm s}^{-1}$. SML samples were removed from the plate using a Teflon wiper (Cunliffe and Wurl,
175 2014) and collected in an acid cleaned and rinsed bottle. Prior to sampling, all equipment was cleaned with acid
176 (10 % HCl) and rinsed in MilliQ and copiously rinsed with seawater directly before samples were taken.
177

178 **2.3.2. DOC analysis**

179 The concentration of dissolved organic carbon (DOC) was determined in samples filtered online (Sartoban ©
180 300; 0.2 μm filters). Subsamples of 10 mL (in duplicate) were transferred to pre-combusted glass ampoules and
181 acidified with H_3PO_4 (final pH = 2). The sealed glass ampoules were stored in the dark at room temperature until
182 analysis. DOC measurements were performed on a Shimadzu TOC-V-CSH (Benner and Strom, 1993). Prior to
183 injection, DOC samples were sparged with CO_2 -free air for 6 min to remove inorganic carbon. A 100 μL aliquot
184 of samples were injected in triplicate and the analytical precision was 2%. Standards were prepared with
185 acetanilide. Analysis of DOC was performed both on SML and the underlying seawater sampled from the
186 zodiac.
187

188 **2.4. Seaspray generation and analysis**

189 **2.4.1 General set-up**

190 The sea spray generator has been characterized and deployed in a number of previous studies and full details are
191 reported in Schwier et al., (2015). Briefly, it consists of a 10 L glass tank, fitted with a plunging jet system for
192 the water. A particle-free air flushing system, placed perpendicular to the water surface at a distance of 1 cm to
193 send a constant airflow across the surface of the water to replicate the effects of wind on the surface of seawater.
194 The sea spray generator was supplied with a continuous flow of seawater collected at a depth of 5 m by an
195 underway seawater circulating system operated with a large peristaltic pump (Verder® VF40 with EPDM hose).

196 The different aerosol instrumentation, including a Time of Flight aerosol chemical speciation monitor (ToF-
197 ACSM), a differential mobility particle sizer (DMPS) coupled with a condensation particle counter (CPC), and
198 an impactor collected submicron particulate matter for offline ion chromatography analysis, sampled from the
199 headspace above the seawater in the tank. Two silica gel dryers were set up in series at the output of the
200 chamber. The aerosol relative humidity was measured continuously and varied from 20% to 40%. The total
201 sampling line length was approximately 2 m with a sampling flow of 5 L/min giving a residence time of less
202 than 30 seconds (Fig. S1). Regular tests were performed to ensure that the system was airtight and free from
203 external aerosol influences.

204 **2.4.2 Aerosol physical and chemical properties**

205 **Size distribution measurements**

206 Particle size distribution and number concentration measurements were obtained using the DMPS-CPC.
207 Measurements were provided approximately every 10 minutes for 25 different size classes ranging from 10 nm
208 up to 500 nm. The size distribution was relatively constant throughout the measurement period giving a principal
209 size mode at 110 nm and a second mode at 300 nm. This size distribution is characteristic of the bubbler
210 seawater generation method (Schwier et al., 2015), and is similar to that from other nascent seawater aerosol



211 generators (Bates et al., 2012), and to that observed in the clean marine boundary layer (Yoon et al., 2007).
212 Although the size distribution remained constant the absolute number concentration varied by a factor of 3 over
213 the sampling period. Details of these changes in aerosol number concentration as well as the associated cloud
214 condensation nuclei activity are detailed in a companion paper (Sellegrì et al. submitted).

215 **Offline PM₁ filter analysis**

216 In parallel to the online aerosol physical and chemical measurements, the generated nascent sea spray aerosol
217 particles were also sampled onto PM₁ quartz filters. Aerosol samples were extracted in MilliQ water by
218 sonication (30 min) for the analysis of the water-soluble components. Extracts were analyzed by ion
219 chromatography for the quantification of the main inorganic ions (Sandrini et al., 2016). An IonPac CS16 3 ×
220 250 mm Dionex separation column with gradient MSA elution and an IonPac AS11 2 × 250 mm Dionex
221 separation column with gradient KOH elution were deployed for cations and anions, respectively. The water-
222 soluble organic carbon (WSOC) content of the extracts was quantified using a TOC thermal combustion analyzer
223 (Shimadzu TOC-5000A). Measurements of the total carbon (TC) content were performed on a filter punch cut
224 before water extraction by a thermal combustion analyzer equipped with a furnace for solid samples (Analytik
225 Jena, Multi NC2100S; Rinaldi et al., 2007). The punch was acidified before analysis to remove inorganic carbon
226 from TC and obtain TOC. Note that for some samples TC was measured also before acidification, allowing the
227 calculation of inorganic carbon content. The amount of inorganic carbon varies between 12 and 71% of TC, and
228 thus the acidification process for sea spray is an important step to follow for TOC measurements. Organic carbon
229 was converted to organic mass using conversion factors of 1.4 for the conversion of WIOC to WIOM, and 1.8
230 for the conversion of WSOC and WSOM, respectively (Facchini et al., 2008).

231 Although filters were only collected on a daily, they provided valuable information on the refractory component
232 of the aerosol population. The volume concentrations measured on the filters were similar to those calculated
233 from the DMPS (Fig. S2).

234 **ToF-ACSM**

235 The ToF-ACSM is based on the same operating principles as the aerosol mass spectrometer (Drewnick et al.,
236 2009). The ToF-ACSM contains a critical orifice, an aerodynamic lens to focus submicron particles into a
237 narrow beam that flows into a differentially pumped vacuum chamber, a heater (600°C) to vaporize particles, an
238 electron emitting tungsten filament (70eV) to ionize the vapor, a compact time-of-flight, mass analyzer (ETOF,
239 TOFWERK AG, Thun, Switzerland) and a discrete dynode detector (Fröhlich et al., 2013). It does not have the
240 ability to size aerosol particles but has the advantage of being more compact and more robust for continuous
241 observations than the AMS (Fröhlich et al., 2013). The ToF-ACSM alternates between sampling ambient air and
242 sampling through a filter in order to subtract the signal due to air.

243 During this experiment the ToF-ACSM was operated in a 2-min filter and 8-min sample mode with a
244 measurement every 10 minutes. The aerodynamic lens transmits particles between 70 nm and 700 nm, making
245 the ACSM approximately a PM₁ measurement. The non-refractory particle material (NR-PM) is defined
246 similarly as in DeCarlo et al. (2006) as aerosol particles that are vaporized using the 600°C resistively heated
247 vaporizer and detected during the instrument sampling interval. The relative ionization efficiency for NH₄ was
248 3.12 and for SO₄ 0.8, determined from calibrations from ammonium sulfate and ammonium nitrate. The



249 temperature of the vaporizer and the size range do not permit efficient detection of sea salt particles. However, in
250 situations of high sea salt concentrations, detection of sea salt ions and related halides have been reported (Bates
251 et al., 2012; Giordano et al., 2017; Ovadnevaite et al., 2011; Schmale et al., 2013, Timonen et al., 2016).
252 Likewise, in this study mass spectral signals associated with sea salt were observed. In addition, the contribution
253 from chloride was very high (72% of the total mass). In some quadrupole ACSM instruments, negative Chl
254 peaks are often observed (Tobler et al., 2020), due to slow evaporation of refractory material from the vaporizer
255 relative to the 30 s switching time of filter and sample. This tends to overestimate the filter measurement and
256 underestimate the sample measurement and can lead to negative values for the difference. However, during these
257 measurements with the ToF-ACSM, negative Chl was not observed due to the long switching times.

258 The typical signature peaks for sea salt aerosol in our instrument were confirmed by atomizing pure aerosol
259 particles generated from sea salt solution (Biokar, synthetic sea salt, lot: 0017475), passing the particles through
260 a silica gel dryer and into the ToF-ACSM instrument. In the default fragmentation table used to assign the
261 signals at individual m/z 's to chemical species (Allan et al., 2004), peaks associated with sea salt were identified
262 as organic aerosol fragments. In order to better represent the measured aerosol composition, we modified the
263 standard fragmentation table by introducing a sea salt species that includes m/z fragments at m/z 23 (Na^+), m/z
264 35 and 37 ($^{35}\text{Cl}^-$, $^{37}\text{Cl}^-$), 58 and 60 (Na^{35}Cl , Na^{37}Cl), and 81 and 83 (NaCl_2 , $\text{NaCl}^{37}\text{Cl}$). For m/z 81, there is
265 overlap with an SO_4 fragment and a correction suggested by Schmale et al. (2013) was applied (Eq.1). This
266 correction accounted for less than 10% of the signal at m/z 81 and 3% of the total sulfate signal.

$$267 \text{frag_SO4}[81] = 81 - \text{frag_organic}[81] - 0.036 \times \text{frag_Na}[23] \quad (\text{Eq.1})$$

268 Quantification of sea salt is difficult in the ToF-ACSM due to inefficient vaporization and a nonlinear
269 contribution to the Na^+ signal from surface ionization on the vaporizer. Therefore, in this work we do not attempt
270 to quantify the sea salt fraction, but instead use the mass spectral information to separate it from the organic
271 aerosols. A standard collection efficiency (CE) of 0.45 was applied to all data obtained from the ACSM
272 (Middlebrook et al., 2012). Regular periods of sampling with a filter in front of the ToF-ACSM were introduced
273 in order to ensure that there was no buildup of material on the vaporizer and that the sampling set up was leak-
274 free.

275 **Positive matrix factorization (PMF)**

276 In order to identify the different organic aerosols present in the sea spray from primary seawater, unconstrained
277 positive matrix factorization, using the SoFi interface (Canonaco et al., 2013) was performed on the ToF-ACSM
278 organic mass spectra. As described above, all sea salt related ions were removed from the organic mass spectral
279 data matrix, giving a total of 116 m/z from 0 up to 150. In addition, we removed the organic signal at m/z 29
280 because it is noisy due to a high background. The PMF solutions were explored up to eight factors. The four-
281 factor solution was chosen, based on correlations with reference mass spectra, and correlations with external
282 time series. The correlations for three to five factor solutions are illustrated in the supplementary material (Fig.
283 S3 to S5). The four identified factors, as well as their mass spectral fingerprints and time series will be discussed
284 in the following sections.



285 **3. Results and discussions.**

286 **3.1. Time evolution of the chemical composition of nascent sea spray**

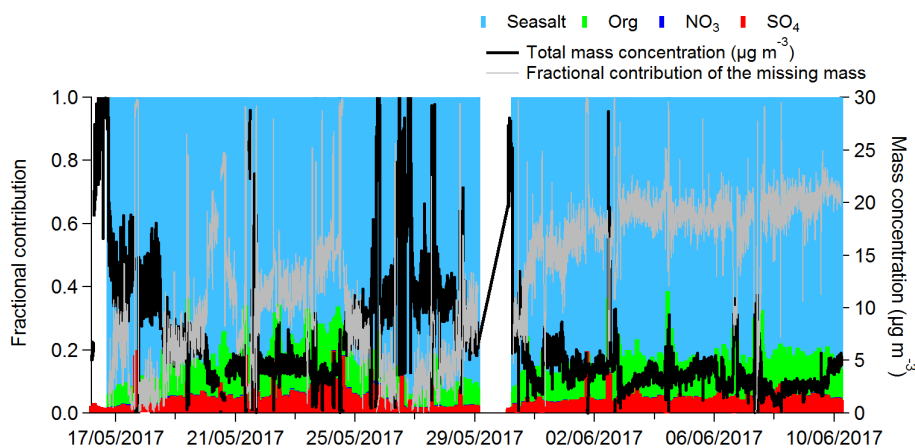
287 Aerosol chemical composition obtained from the submicron offline filter measurements showed an average mass
288 contribution is listed in Table 1. The soluble inorganic species concentrations were mostly found with
289 proportions similar to the reference average seawater composition (Seinfeld and Pandis, 2006). However,
290 enrichment in K^+ (69% of which was not explained by the average seawater composition) and a slight
291 enrichment of Ca^{2+} was measured toward the end of the campaign (17% of Ca^{2+} was not explained by reference
292 seawater composition from the 28th of May onward). In contrast, the magnesium was slightly depleted (20% less
293 than expected in reference seawater composition) but less towards the end of the campaign. Filter-based organic
294 matter (OM) was evenly composed of WIOM (14±5% of total mass) and WSOM (9%±5% of total mass), which
295 contrasts with previous studies where organic matter in ambient marine aerosol was almost exclusively
296 composed of WIOM (Facchini et al., 2008). However, these previous studies were conducted during
297 phytoplankton bloom events of the Northern Atlantic Ocean, where POC is usually enhanced. Given that the
298 Mediterranean Sea is characterized by oligotrophic conditions during PEACETIME, it could explain the
299 relatively low contributions of WIOM.

300 **Table 1. Concentrations of different chemical species in PM1 primary seawater aerosols measured using offline**
301 **analysis of filters and online measurements from the ACSM.**

offline analysis of filters ($\mu\text{g m}^{-3}$)	%	Non-refractory PM1 (ACSM) ($\mu\text{g m}^{-3}$)	%		
SO_4^{2-}	1.53 ± 0.7	7%	SO_4	0.18 ± 0.15	3.2%
Na^+	4.86 ± 1.9	21%	NO_3	0.02 ± 0.02	0.1%
Cl^-	10.4 ± 4.2	45%	NH_4	0.04 ± 0.11	1.2 %
Ca^{2+}	0.19 ± 0.07	0.07%	Seasalt	5.86 ± 5	84%
K^+	0.11 ± 0.05	0.5%	Org	0.54 ± 0.38	9.3%
Mg^+	0.50 ± 0.22	2%			
WIOM	3.13 ± 1.12	14M			
WSOM	2.02 ± 1.26	9M			

302

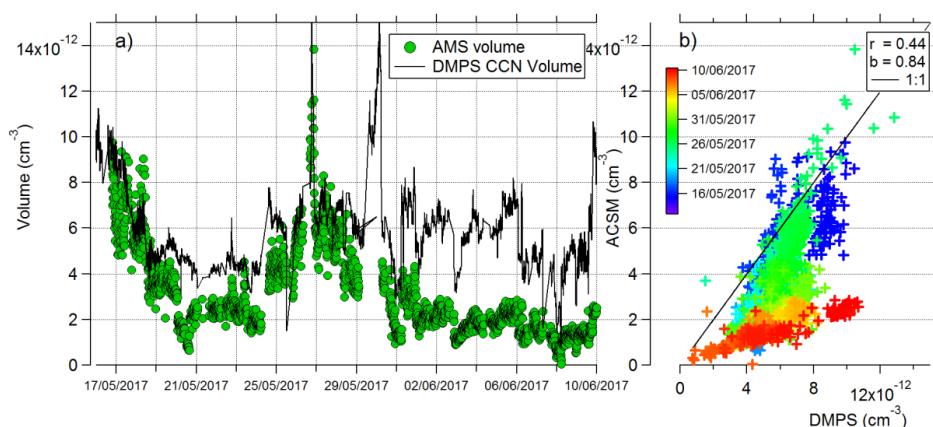
303 The chemical composition of SSA measured by the ACSM is shown in Fig. 2 and listed in Table 1 and was
304 primarily composed of Sea Salt aerosol (determined from the signals at m/z 23 (Na^+), 35 (Cl^-), 37(Cl^-)
305 58($NaCl^+$), 60($NaCl^+$), 81($NaCl$) Na^+ (84% ±15 %) followed by SO_4 concentrations at 3 %, and 9% organic
306 matter.



307

308 **Figure 2: Time series of the fractional contribution of different species to the ToF-ACSM signal, as well as the total**
 309 **mass concentrations measured by the ACSM (black), and the missing fraction (RefrMass) in grey.**

310 In order to determine how representative the ACSM PM1 measurements were of the total PM1 mass, the total
 311 ACSM PM1 mass concentration was converted into volume concentration (dividing organic mass concentrations
 312 by a density value of 1.2 g cm^{-3} , and inorganic and sea salt components by 1.75 g cm^{-3} (Seinfeld and Pandis,
 313 2006). This value was compared to the volume concentration measured by the DMPS-CPC, giving a correlation
 314 (R) of 0.44, and slope (b) of 0.84 (Fig. 3). The agreement is relatively good in the first part of the transect, but
 315 the difference between the ACSM-derived volume and the DMPS-derived volume increases over time. The
 316 refractory material (Refr.) not measured by the ACSM is calculated as the difference between DMPS volume
 317 concentration and ACSM volume concentration.



318

319 **Figure 3 Comparison between the ACSM and the DMPS volume concentration ($\#/ \text{cm cm}^{-3}$).**

320 The difference between the volume concentrations measured by the ACSM and SMPS were $44\% \pm 22\%$. NaCl
 321 concentrations measured with the ACSM were in good agreement with the NaCl concentrations measured from
 322 filters except during periods corresponding notably to the presence of the non-measured refractory mass (Fig

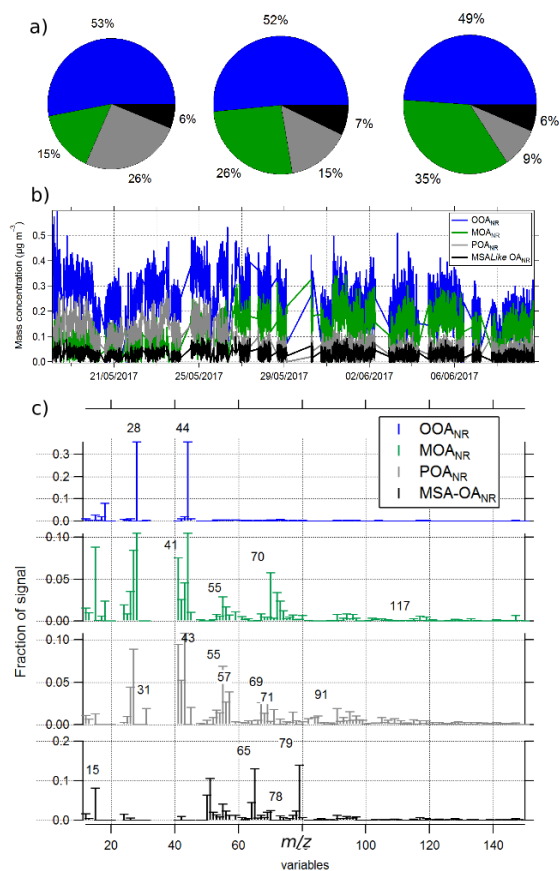


323 S6). This might suggest that the ability of the ACSM to measure NaCl particles depends on how NaCl is
324 associated with other compounds in the sea spray. Comparing this Refr. particle type to the different species
325 measured on the filters shows that it is reasonably correlated to the filter-based analysis of Mg^{2+} , Ca^{2+} , and NaCl.
326 Hence, it is possibly made of a mixture of carbonates from Ca^{2+} , Mg^{2+} and sea salt . (Fig S7). The PM1 mass
327 concentrations of OM calculated from the filters were additionally compared with the total OM measured from
328 the ACSM (OM_{ACSM}) (Fig. S8), the OM_{ACSM} was on average 80% lower than the total filter OM, indicating that
329 part of the refractory mass also contains organic matter. The temporal variation of the WSOM agreed better with
330 that of OM_{ACSM} than that of WIOM.

331 OM_{ACSM} varied from 0.2 to 1 $\mu g m^{-3}$, with higher concentrations measured in the North Western part of the ship
332 track. In the following section, we analyze in more detail the different organic aerosol species present in the
333 SSA samples and determine to what extent they are related to seawater biogeochemical properties.

334 3.2. Marine organic aerosol speciation

335 As explained in section 2 (Methodology), PMF was used to separate four organic factors. Based on correlations
336 with reference mass spectra we identified these factors as: an oxidized organic aerosol (OOA_{NR}), a somewhat
337 oxidized OA containing mixed amino acid and fatty acid signatures (MOA_{NR}); primary organics containing
338 aliphatic signature peaks as well as several peaks corresponding to fatty acids signatures (POA_{NR}), and a
339 methanesulphonic acid-like type OA ($MSA-OA_{NR}$) (Fig. 4). The correlations of each of the identified factors
340 with reference mass spectra are illustrated in Fig. S4. The OOA_{NR} contributed $51\% \pm 2\%$ to OA and had
341 signature peaks with high m/z 44 and m/z 28. It did not contain any other m/z values that might suggest a
342 contribution from other species. The O/C ratio of the OOA_{NR} fraction was 1.6 (calculated using the method
343 described in Canagaratna et al., 2015), which is significantly higher than the average O/C ratio of LV-OOA
344 found in terrestrial ambient aerosols (0.8) (Canagaratna et al., 2015). High O/C ratios have been reported in
345 ambient studies where the carbonate species were thought to be measured by the ACSM (Bozzetti et al., 2017,
346 Vlachou et al., 2019). Thus the high O/C ratio observed for the OOA_{NR} organic class is not necessarily the
347 signature of the oxidation or processing of the primary organic matter.



348

349 **Figure 4 a) The contribution of the different organic factors the PEACETIME ship campaign, b) The mass**
350 **concentrations of each factor (OOA_{NR}, MOA_{NR}, POA_{NR} and MSA OA_{NR}) as a function of time, c) the mass spectra of**
351 **the factors.**

352 The second most dominant species was defined as a marine organic aerosol (MOA_{NR}). This factor contributed
353 15% to the total OOA_{NR} at the start of the campaign and then increased to 28% and 35% later on in the campaign
354 (Fig. 4a). This MOA_{NR} factor contained several mass peaks associated with amino acids (AA) reported in
355 reference mass spectral signatures of leucine and valine respectively (Schneider et al., 2011). AA signature
356 peaks were identified at m/z 41 ($C_2H_3N^+$), 70, 98, 112 ($C_6H_{12}N_2^+$), 115, ($C_5H_9NO_2$), 117 ($C_5H_{11}NO_2$), 119
357 ($C_4H_9NO_3$), 131 ($C_6H_{13}NO_2$) and were similar to signature peaks that had been identified in previous studies by
358 Schmale et al. (2013) in ambient marine aerosols and by Schneider et al. (2011) during a series of laboratory
359 studies on different AA. Similar marker m/z 's were present for fatty acid species such as those palmitic and
360 oleic acid (Alfarra, PhD thesis 2004)). The MOA_{NR} factor had an O/C of 0.53 and an H/C of 1.39, hence much
361 less oxidized than the OOA_{NR} type. These values are intermediate between those often calculated for low
362 volatility, and semi-volatility OOA_{NR} in the ambient atmosphere (Canagathna et al., 2015), and are similar to
363 those identified by Schmale et al., 2013 for an amino acid type aerosol (O/C 0.35 and H/C 1.65) detected in an
364 ambient aerosol.



365 The third most prominent factor was identified as a primary organic aerosol (POA_{NR}) and contributed 26% to the
366 total organics at the start of the campaign and decreased to 9% near the end of the campaign (Fig. 4b). This
367 factor contained typical aliphatic signatures and had little contribution from m/z 44. The mass spectral signature
368 of POA_{NR} factor correlated well with reference mass spectra of leucine (R=0.56) and valine (r=0.51) but also
369 with fatty acid mass spectra, oleic (r=0.69), and palmitic acid (R= 0.74). The O/C ratio of this POA_{NR} was 0.1
370 and the H/C was 1.64, which is typical for values of primary organic aerosol in the ambient atmosphere. The
371 POA_{NR} factor identified in this work, as well as the H/C ratios, was similar to the aliphatic rich organic aerosol
372 species measured in contained wave chamber experiments during a phytoplankton bloom (Wang et al., 2015).
373 Once the bloom passed the H/C of these aerosol particles decreased, and it was hypothesized that the primary
374 organics were transformed through microbial activity in the water. During the PEACETIME campaign, the
375 POA_{NR} factor had highest concentrations at the start of the field campaign and then later decreased to constant
376 values. This decrease in POA_{NR} was accompanied by an increase in the more oxidized MOA_{NR}.

377 The last factor, MSA-OA_{NR}, contributed 6% ± 1% and contained typical signature peaks at m/z 65 (HSO₂⁺), 79
378 (CH₃SO₂⁺), and 96 (CH₄SO₃⁺) similar to the mass spectral signatures identified by Timonen et al., (2016) in
379 Antarctica. However, unlike previously measured ambient MSA-like species (Schmale et al., 2013 Mallet et al.,
380 2019) it contained little or no oxygenated peaks at lower masses (m/z 43, 44, 45) making it impossible to
381 calculate an O/C ratio. However the H/C ratio of 1.12 was similar to 1.2 measured by Ovadnevaite et al. (2011),
382 but lower than the reported 1.6 by Schmale et al. (2011) for MSA-OA_{NR}, both detected in ambient aerosol. The
383 presence of an MSA-OA in nascent sea spray generated in the present study suggests that this compound is
384 already present in the seawater, and not only produced from gas-phase DMS emissions and oxidation in the
385 atmosphere. The Mediterranean Sea experiences a high level of radiation (Mermex 2011), and could also explain
386 the presence of MSA-like compounds from DMS oxidation within the seawater.

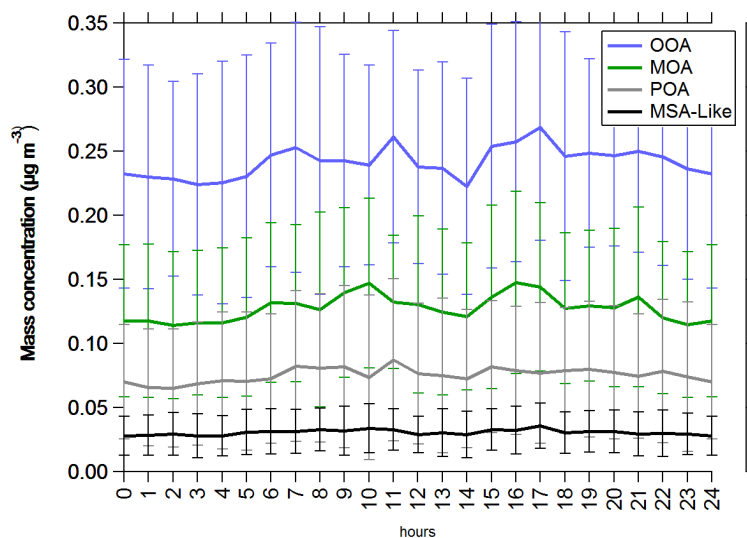
387 AA containing OA have been measured at a number of coastal sites, and their formation in the ambient
388 atmosphere is similar to that of MSA, where the AA are formed from the gas-phase partitioning of amines such
389 as trimethylamine or dimethylamine into the particulate phase (Facchini et al., 2008). However, a small number
390 of studies have identified these aerosol particle types directly from bubble bursting during controlled chamber
391 experiments (Dall'Osto et al., 2019; Kuznetsova et al., 2005; Decesari et al. 2019). These AA OA signatures
392 were detected during measurements made on the east coast of America, or in the Arctic (Dall'Osto et al, 2019),
393 and also during controlled wave chamber experiments (Wang et al, 2015).

394 In our experimental setup, the short time between particle generation and analysis (less than 30 seconds) does
395 not allow for the formation of secondary aerosol through the partitioning of gas-phase species into the particle
396 phase. Since these amino acid signatures are internally mixed with signatures for several different species, we
397 assume that they are present in the organic matter of the seawater, similar to conclusions made by Dall'Osto et
398 al. (2019).

399 OOA_{NR} and MOA_{NR} factors had a slight diurnal variation with increases during the early hours of the morning
400 and again in the afternoon (Fig 5). However given the low magnitude of the diurnal variation it is unlikely that
401 photochemical processes had a significant influence on the production of these species, and they are more likely
402 the result of processing of organic matter by microorganisms.



403



404

405 **Figure 5: Diurnal variation of the four PMF organic factors chosen to represent the measured non refractory organic**
406 **aerosol: average and standard deviation of the measurements during the whole PEACETIME cruise**

407 3.3. The sources and formation pathways of marine organic aerosol species

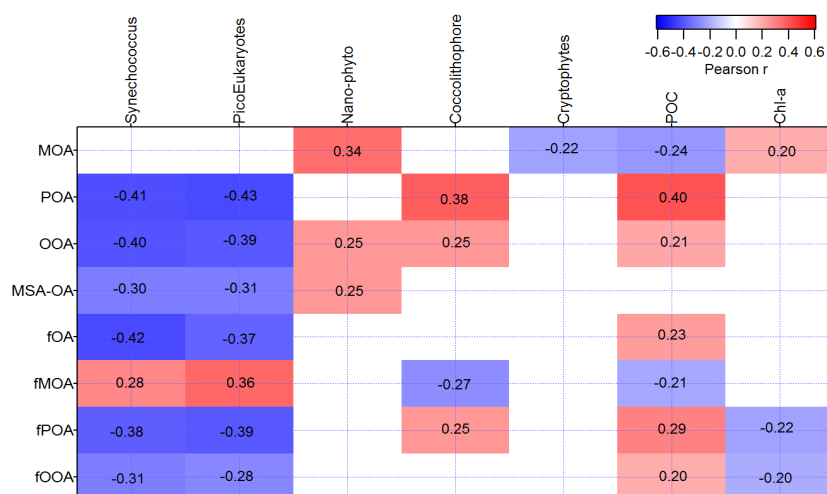
408 In several large-scale climate models *Chl-a* is used as a proxy of phytoplankton biomass to predict the organic
409 fraction of sea spray. In this study, the measured *Chl-a* in the underway surface seawater was low and had little
410 variability ($0.07 \pm 0.013 \text{ mg m}^{-3}$), therefore making it difficult to extract any significant relationship between our
411 measured organic mass fractions and the measured *Chl-a*. No significant correlations were observed between the
412 mass concentrations of the OM, (measured by either the ACSM (OM_{ACSM}) or on filters ($\text{OM}_{\text{filter}}$
413 ($\text{WIOM}+\text{WSOM}$)) and *Chl-a* concentrations, nor between the fraction of these two organic classes to the total
414 seaspray mass and *Chl-a* (not shown). The fact that satellite-based, concurrently measured *Chl-a* may not be the
415 best surrogate for marine organic aerosol has been highlighted in previous studies (Rinaldi et al., 2013). This is
416 especially the case when little phytoplankton biomass is present. Therefore it is important to identify other
417 marker species or processes that can be used to correctly link seawater chemical composition, biological activity,
418 and the organic fraction in the seawater aerosol that can represent up to 20% of the total submicron sea spray
419 mass in oligotrophic waters.

420 In a companion paper, we illustrate that the total number of sea spray particles measured by the DMPS was
421 correlated to the nanophytoplankton cell abundance (NanoPhyto) ($r=0.33$, $n=501$, $p < 0.001$), (Sellegri et al.
422 submitted). The hypothesis behind the dependence of the sea spray number concentration on NanoPhyto is that
423 organic matter released by NanoPhyto influences the surface seawater (SSW) surface tension, and therefore the
424 bubble lifetime that drives the number of film drops ejected to the atmosphere.



425 **3.3.1. High time resolution correlations**

426 In this section we will investigate the dependence of each of the organic classes identified in sea spray to the
427 SSW biogeochemical properties. The relationships of the total organic mass concentrations and the fractional
428 organic contributions to the seawater biochemistry were investigated (Fig; 6).



429

430 **Figure 6: Pearson correlation matrix showing the agreement of the four different organic factors (MOA_{NR}, POA_{NR}, OOA_{NR} and MSA-OA_{NR}) and their fraction to the total sea spray mass (fMOA, fPOA, fOOA and fOA) with several**
431 **phytoplankton functional group abundance (cell. cm³) (Synechococcus, PicoEukaryotes, NanoEukaryotes (Nano-**
432 **Phyto), Coccolithophore (Coccolith), Cryptophytes), total Chl-a (mg.m⁻³) and POC (µM) in the sampled seawater**
433 **during the whole campaign. Sample number = 461, Correlations with R values < 0.16 had significance values lower**
434 **than 0.001 and were therefore left blank.**
435

436 MOA_{NR} was strongly linked to NanoPhyto ($r=0.34$), as was MSA-OA_{NR} and OOA_{NR} but with less significance
437 ($r=0.25$). Therefore, these organic classes follow the total sea spray mass and number behavior, as illustrated in
438 Sellegri et al., (submitted). The hypothesis of organic matter influencing the surface tension of seawater, bubble
439 lifetime, and the number of film drops, is therefore linked to this specific class of organic matter. Fatty acids,
440 present in the MOA_{NR} and OOA_{NR} spectra, have been reported to be enriched in the SML (Cunliffe et al., 2012)),
441 which would explain their impact on the bubble bursting process. POA_{NR} species are instead significantly
442 correlated with particulate organic carbon concentrations [POC] ($r=0.40$), and Coccolithophore like abundance
443 ($r=0.38$) (Eq.2). A relationship between Coccolithophore-like cell abundance and [POC] is likely linked to the
444 ability of the coccolithophores or similar groups of phytoplankton to secrete large amounts of sticky carbon
445 which can result in the formation of gels and POC (Engel et al., 2004). As the time variation of POA_{NR} does not
446 follow that of total sea spray mass, it is possible that POA is not linked to film drops formation and is ejected
447 into the atmosphere via separate mechanisms (such as jet drops). The time series of OOA_{NR} had positive
448 relationships with NanoPhyto ($r=0.25$), but also with coccolithophore-like cell abundances ($r=0.25$) and [POC]
449 ($r=0.21$) and hence OOA_{NR} seem to have an intermediate behavior between POA_{NR} and MOA_{NR}. All organic
450 classes except MOA_{NR} are anticorrelated to the small classes of phytoplankton (picoeukaryotes and



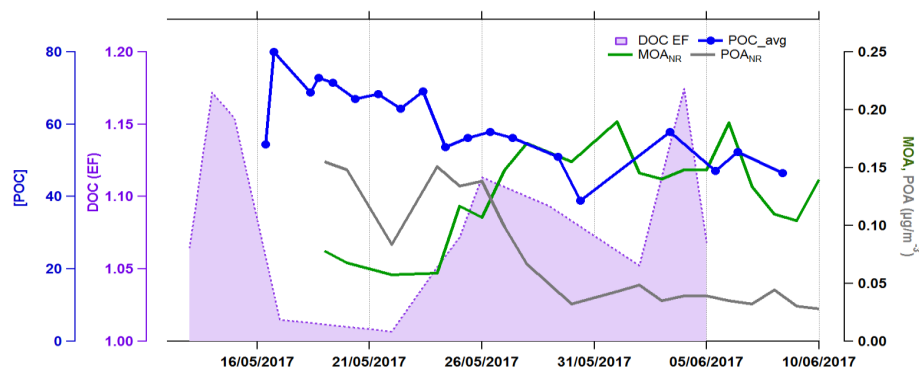
451 synechococcus). This anticorrelation could be the result of the competition for nutrients between these small
452 cells and the larger ones that rather drive the POC content.

453

454 Except for MOA_{NR} , all correlations for the absolute mass of these different types of organic matter are also
455 observed when the fractional contribution of these species to the total mass of SSA (determined from the DMPS)
456 are considered, although less significant (lower part of Fig.6). However, for MOA_{NR} species, correlations with
457 Nano-Phyto no longer hold if the fractional contribution of these species to the total mass of sea spray is
458 considered. Instead, fMOA is correlated to picoeukaryotes and synechococcus. This is likely due to the strong
459 anticorrelation of the fraction of all other organic classes with these small classes of phytoplankton. At low
460 picoeukaryotes and Synechococcus cell abundances, fPOA, fOOA, and fMSA-OA are higher, artificially
461 decreasing the proportion of fMOA to the rest of the organic matter.

462 3.3.2. Filter-based resolution correlations

463 Since the non-refractory organic components analyzed using the ACSM technique are only a fraction of the
464 marine organic mass, we investigate the relationships between off-line filter-based organic compounds and
465 seawater biogeochemical properties.



466

467 **Figure 7. Time series of the DOC enrichment factor (EF), [POC] concentrations, and PMF organic factors MOA and**
468 **POA.**

469 Filter-based organic fractions are also compared to seawater properties at the filter sampling time resolution. The
470 organic mass concentration from filters is correlated to the coccolithophore cell abundance ($R=0.88$, $n=13$). The
471 fraction of OM to total mass analyzed on filters (OMSS) was also correlated to coccolithophore cell abundance
472 ($R=0.72$, $n=13$) and POC ($R=0.6$, $n=13$). This indicates that the total organic matter present in sea spray behaved
473 similarly to the non-refractory POA and OOA analyzed by the ACSM. Previous studies observed a connection
474 between seawater POC and SSA organic fraction. Facchini et al. (2008) found that WIOM in SSA was related to
475 seawater POC derived from microgels. Furthermore, during mesocosm bubbling experiments using *Emiliania*
476 *huxleyi* cultures and low heterotrophic prokaryote abundance counts, O'Dowd et al., (2015) suggested that the
477 aggregation of DOM into POC in the form of insoluble gel-colloids was the driving force behind the enrichment
478 of organic matter into submicron SSA. The authors hypothesized that the organic fraction of SSA can be
479 controlled either by DOC or POC, depending on the biological state of the waters.



480 Measurements of DOC in the SML and underlying seawater were performed daily, as well as surface seawater
481 bacterial total counts from daily CTD samples (surface water at 5m depth). DOC was slightly enriched in the
482 SML compared to the underlying seawater, with enrichment factors varying between 1 and 1.2 (Fig. 7). The
483 filter-based total organic content of sea spray aerosol was not correlated to DOC or total bacterial count in the
484 SML, neither was OMSS. However we observe that MOA_{NR} was correlated to the enrichment of DOC in the
485 SML ($R=0.55$, $n=9$, $p=0.1$), suggesting again that MOA_{NR} is likely linked to organic matter present in the
486 SML. The correlation between MOA and DOC enrichment in the SML suggests that the fraction of DOC which
487 is enriched in the SML contains lipids and amino acids found in the MOA_{NR} fraction. Although MOA_{NR} is an
488 oxidized organic class, it does not seem to be the result of the bacterial production (BP) of organic matter in the
489 seawater. We actually found a significant anticorrelation between MOA_{NR} and the bacterial production ($R=-0.82$,
490 $n=10$), indicating that MOA could instead be consumed by this process, while OMSS, positively correlated to
491 BP ($R=0.68$, $n=10$), would be a product of BP.

492 3.3.3. Predicting organic matter in sea spray from seawater biogeochemical properties

493 By combining relationships between filter-based chemical analysis, ACSM organic source apportionment and
494 seawater properties, it is possible to propose a general relationship that can be used to predict the different
495 fractions of organic matter in the nascent sea spray emitted from oligotrophic seawaters. These different organic
496 fractions may have different atmospheric properties related to their climate impact, such as ice nuclei properties
497 (Trueblood et al. in prep). We chose to parameterize the organic fractions of sea-spray rather than computing
498 organic mass fluxes, for an easier implementation in models that already have an inorganic sea spray source
499 function. However, as shown in the preceding section, the total mass of sea spray is significantly influenced by
500 SSW biology, and we recommend that the biology dependent sea spray number fluxes modulation computed in
501 Sellegri et al. (submitted) is applied before biology-dependent organic fractions are calculated.

502 The non-refractory organic fraction of nascent sea spray can be predicted with three different equations, with
503 $MSA-OA_{NR}$ being a negligible fraction of the total sea spray mass:

$$504 \text{fPOA} = 0.0002 [\text{POC}] - 0.001 \quad R = 0.29, n=459, p < 0.001 \quad \text{Eq. 4}$$

$$505 \text{fOOA} = 0.0002 [\text{POC}] + 0.02 \quad R = 0.20, n=478, p < 0.001 \quad \text{Eq. 5}$$

$$506 \text{fMOA} = 4.5 \cdot 10^{-6} \times (\text{picoeukaryotes}) + 0.009 \quad R = 0.36, n=459, p < 0.001 \quad \text{Eq. 6}$$

507 By subtracting all NR organic concentrations (ACSM measured) from the total filter-based organic
508 concentration, we obtain the refractory fraction of the organic matter (RefractOrg). This fraction dominates the
509 organic matter in sea spray. The fraction of RefractOrg to the total mass analyzed on filters (fRefraOrg) is
510 correlated to coccolithophores ($R=0.82$, $n=11$, $p=0.001$) and POC concentrations ($R=0.81$, $n=10$, $p=0.001$),
511 similarly to the POA_{NR} and OOA_{NR} fractions of the sea spray, but with a better correlation to POC. Since POC
512 values are more available than coccolithophore numbers in models or satellite data, fRefraOrg can be computed
513 as follows:

$$514 \text{fRefraOrg} = 0.005 \times [\text{POC}] - 0.11 \quad \text{Eq. 7}$$



515 These relationships apply to the ranges of POC and picoeukaryotes measured during the PEACETIME cruise,
516 hence they may be applicable to other oligotrophic waters. If larger ranges of seawater biogeochemical
517 properties are considered in the future though, fractions of organic classes should be parameterized as
518 logarithmic laws asymptotic to 1, in order to take into account the saturation of the organic fraction at 1 for the
519 largest POC values.

520 **4. Conclusions**

521 The primary objective of this experiment was to study the relationships between sea spray chemical properties
522 and those of seawater. This work presents a unique dataset, which describes the first deployment of a ToF-
523 ACSM to characterize, in a continuous way, the organic fraction present in sea spray aerosol generated from
524 Mediterranean surface seawater. The non-refractory part of the organic content of sea spray was characterized by
525 low organic content and low variability along a 4300 km transect. Yet, using a positive matrix factorization on
526 the ACSM organic mass spectra, it was possible to extract signatures for fatty acids, amino acids, and marine
527 primary organic aerosols in non-refractory nascent sea spray. We identified four organic families: two were
528 composed of mixtures of amino acids and fatty acids (a primary aerosol POA_{NR} , and a slightly oxidized MOA_{NR}
529 factor), and two were identified as more oxidized organic aerosol (OOA_{NR} and $MSA_{OA_{NR}}$). The POA_{NR} factor
530 was similar to that observed in wave chamber experiments and correlated well with POC concentrations in the
531 seawater, as did the OOA_{NR} and $MSA_{OA_{NR}}$. The MOA_{NR} concentrations had a different behavior and
532 correlated well with the nano-phytoplankton cell abundance in the seawater, and also with the total sea spray
533 number concentration and DOC enrichment in the surface microlayer. It is hypothesized that MOA_{NR} has surface
534 tension properties that influence the bubble bursting process and the resulting number of film drops ejected to the
535 atmosphere. In contrast, the fraction of POA, OOA and MSA classes are not connected to the sea spray number
536 concentration, but are linked to POC of the bulk surface seawater and more likely emitted with a different
537 process such as through jet drops.

538 Off-line chemical analysis of the submicron nascent sea spray provided a general view of the total organic
539 content of these particles, showing that a large part of the organic matter was refractory (to vaporization at
540 600°C) and thus not detected by the ACSM. However, this refractory organic matter within the nascent sea spray
541 was transferred to the atmospheric aerosol phase similarly to the POA_{NR} concentration found from the ACSM
542 analysis, being significantly correlated to the POC content of the bulk seawater.

543 This work illustrates the value of continuous aerosol chemistry and physical characterization of the nascent sea
544 spray aerosol in parallel with other biogeochemical measurements in surface seawater. It also illustrates that
545 even under oligotrophic conditions, seawater biogeochemical properties influence the type and concentration of
546 marine organic aerosols and therefore their ability to act as cloud condensation nuclei or ice nuclei. We provide a
547 parameterization of the different marine organic components of nascent sea spray as a function of seawater
548 biogeochemical properties typical for oligotrophic conditions in LNLC regions of the ocean that represents 60%
549 of the global ocean. Such parameterization used in models should allow a better prediction of the impact of
550 living marine organisms on these properties in a future climate.



551 **Data availability:** Underlying research data are being used by researcher participants of the “Peacetime”
552 campaign to prepare other manuscripts, and therefore data are not publicly accessible at the time of publication.
553 Data will be accessible (<http://www.obs-vlfr.fr/proof/php/PEACETIME/peacetime.php>, last access: 22 June
554 2020) once the special issue is completed (all papers should be published by fall 2020). The policy of the
555 database is detailed here <http://www.obs-vlfr.fr/proof/dataconvention.php> (last access: 22 June 2020).

556 **Acknowledgments**

557 This study is a contribution to the PEACETIME project (<http://peacetime-project.org>), a joint initiative of the
558 MERMEX and ChArMEx components supported by CNRS-INSU, IFREMER, CEA, and Météo-France as part
559 of the programme MISTRALS coordinated by INSU. PEACETIME was endorsed as a process study by
560 GEOTRACES. PEACETIME cruise <https://doi.org/10.17600/17000300>. Sea2Cloud was endorsed by
561 SOLAS; We thank the captain and the crew of the RV Pourquoi Pas ? for their professionalism and their work at
562 sea.

563 **Author contributions:** CG and KD designed the PEACETIME project. KS designed the experiments
564 specifically used in this manuscript. KS and AN performed the measurements aboard the ship. MT, GG, NH, JD,
565 IO, F V-W, A.E and BZ were responsible for collecting and analyzing the biogeochemical parameters in either
566 the seawater or in the surface microlayer. MR analyzed the offline filter measurements. EF analyzed the ACSM
567 data with input from LW and ASHP. EF and KS prepared the manuscript with contributions from all authors.

568 **References:**

- 569 Allan, J.D., Delia, A.E., Coe, H., Bower, K.N., Alfarra, M.R., Jimenez, J.L., Middlebrook, A.M., Drewnick, F.,
570 Onasch, T.B., Canagaratna, M.R. A generalised method for the extraction of chemically resolved mass
571 spectra from Aerodyne aerosol mass spectrometer data. *J. Aerosol Sci.* 35, 909–922.
572 <https://doi.org/10.1016/j.jaerosci.2004.02.007>, 2004
- 573 Bates, T., Quinn, P., Frossard, A., Russell, L., Hakala, J., Petäjä, T., Kulmala, M., Covert, D., Cappa, C., Li, S.
574 Measurements of ocean derived aerosol off the coast of California. *J. Geophys. Res Atmos*
575 117. <https://doi.org/10.1029/2012JD017588>, 2012
- 576 Benner R, Strom M. A critical evaluation of the analytical blank associated with DOC measurements by high
577 temperature catalytic oxidation. *Mar Chem* 41:153–160, [https://doi.org/10.1016/0304-4203\(93\)90113-](https://doi.org/10.1016/0304-4203(93)90113-3)
578 3, 1993
- 579 Boss, E., M. Picheral, T. Leeuw, A. Chase, E. Karsenti, G. Gorsky, L. Taylor, W. Slade, J. Ras, H. Claustre. The
580 characteristics of particulate absorption, scattering and attenuation coefficients in the surface ocean;
581 Contribution of the Tara Oceans expedition, *Methods in Oceanography*. 7, 52–62,
582 <https://doi.org/10.1016/j.mio.2013.11.002>, 2013
- 583 Burrows, S. M., Ogunro, O., Frossard, A. A., Russell, L. M., Rasch, P. J., and Elliott, S. M.: A physically based
584 framework for modeling the organic fractionation of sea spray aerosol from bubble film Langmuir
585 equilibria, *Atmos. Chem. Phys.*, 14, 13601–13629, <https://doi.org/10.5194/acp-14-13601-2014>, 2014.
- 586 Blanchard, D.C., Woodcock, A.H. The production, concentration, and vertical distribution of the sea-salt aerosol.
587 *The. N. Y. Acad. Sci.* 338, 330–347. <https://doi.org/10.1111/j.1749-6632.1980.tb17130.x>, 1980



- 588 Bozzetti, C., I. El Haddad, D. Salameh, K. R. Daellenbach, P. Fermo, R. Gonzalez, M. C. Minguillon, Y. Iinuma,
589 L. Poulain, M. Elser, E. Muller, J. G. Slowik, J. L. Jaffrezo, U. Baltensperger, N. Marchand, and A. S.
590 H. Prevot. Organic aerosol source apportionment by offline-AMS over a full year in Marseille, *Atmos.*
591 *Chem. Phys.*, 17, 8247–8268, <https://doi.org/10.5194/acp-17-8247-2017>, 2017
- 592 Canagaratna, M., Jimenez, J., Kroll, J., Chen, Q., Kessler, S., Massoli, P., Hildebrandt Ruiz, L., Fortner, E.,
593 Williams, L., Wilson, K., 2015. Elemental ratio measurements of organic compounds using aerosol
594 mass spectrometry: characterization, improved calibration, and implications. *Atmos. Chem. Phys.*, 15,
595 253–272, <https://doi.org/10.5194/acp-15-253-2015>, 2015.
- 596 Canonaco, F., Crippa, M., Slowik, J., Baltensperger, U., Prévôt, A.S., 2013. SoFi, an IGOR-based interface for
597 the efficient use of the generalized multilinear engine (ME-2) for the source apportionment: ME-2
598 application to aerosol mass spectrometer data. *Atmos. Meas. Tech.*, 6, 3649–3661,
599 <https://doi.org/10.5194/amt-6-3649-2013>, 2013.
- 600 Cetinic, M. J. Perry, N. T. Briggs, E. Kallin, E. A. D'Asaro, and C. M. Lee, Particulate organic carbon and
601 inherent optical properties during 2008 North Atlantic bloom experiment, *J. Geophys Res-Oceans;*
602 *Geophysical Research: Oceans*, 117 (6), doi:10.1029/2011JC007771, 2012.
- 603 Christaki, U., Courties, C., Massana, R., Catala, P., Lebaron, P., Gasol, P., and Zubkov, M. V. Optimized routine
604 flow cytometric enumeration of heterotrophic flagellates using SYBR Green I, *Limnol. Oceanogr.*
605 *Meth*, 9, 329–339. <https://doi.org/10.4319/lom.2011.9.329>, 2011.
- 606 Cunliffe, M., Engel, A., Frka, S., Gasparovic, B., Guitart, C., Murrell, C., Salter, M., Stolle, C., Upstill-Goddard
607 R., and Wurl, O. Sea surface microlayers: A unified physiochemical and biological perspective of the
608 air-ocean interface. *Prog Oceanogr*, 109, 104–116, <https://doi.org/10.1016/j.pocean.2012.08.004>, 2013.
- 609 Cunliffe, M., and Wurl, O. Guide to best practices to study the ocean's surface. Plymouth, UK, Marine
610 Biological Association of the United Kingdom for SCOR, 118pp. (Occasional Publications of the
611 Marine Biological Association of the United Kingdom). <http://hdl.handle.net/11329/261>, 2014;
- 612 Dall'Osto, M., Airs, R.L., Beale, R., Cree, C., Fitzsimons, M.F., Beddows, D., Harrison, R.M., Ceburnis, D.,
613 O'Dowd, C., Rinaldi, M. Simultaneous detection of alkylamines in the surface ocean and atmosphere of
614 the Antarctic sympagic environment. *ACS Earth Space Chem.* 3, 854–862.
615 <https://doi.org/10.1021/acsearthspacechem.9b00028>, 2019
- 616 Decesari, S., Paglione, M. Rinaldi, M., Dall'Osto, M., Simó, R., Zanca, N., Volpi, F., Facchini, M-C., Hoffmann,
617 T., Götz, S., Kampf, K.J, O'Dowd, C., Ovadnevaite, J., Ceburnis, D., and Tagliavini, E. Shipborne
618 measurements of Antarctic submicron organic aerosols: an NMR perspective linking multiple sources
619 and bioregions *Atmos. Chem. Phys. Discuss.*, <https://doi.org/10.5194/acp-2019-888>, 2019
- 620 Drewnick, F., Hings, S. S., Alfarra, M. R., Prevot, A. S. H., and Borrmann, S.: Aerosol quantification with the
621 Aerodyne Aerosol Mass Spectrometer: detection limits and ionizer background effects, *Atmos. Meas.*
622 *Tech.*, 2, 33–46, <https://doi.org/10.5194/amt-2-33-2009>, 2009.
- 623 Engel, A., Delille, B., Jacquet, S., Riebesell, U., Rochelle-Newall, E., Terbrüggen, A., Zondervan, I. Transparent
624 exopolymer particles and dissolved organic carbon production by *Emiliania huxleyi* exposed to



- 625 different CO₂ concentrations: a mesocosm experiment. *Aquat. Microb. Ecol.* 34, 93–104.
626 DOI: 10.3354/ame034093, 2004
- 627 Facchini, M.C., Rinaldi, M., Decesari, S., Carbone, C., Finessi, E., Mircea, M., Fuzzi, S., Ceburnis, D.,
628 Flanagan, R., Nilsson, E.D. Primary submicron marine aerosol dominated by insoluble organic colloids
629 and aggregates. *Geophys. Res. Lett.* 35.
630 <https://doi.org/10.1029/2008GL034210>, 2008
- 631 Fröhlich, R., Cubison, M. J., Slowik, J. G., Bukowiecki, N., Prévôt, A. S. H., Baltensperger, U., Schneider, J.,
632 Kimmel, J. R., Gonin, M., Rohner, U., Worsnop, D. R., and Jayne, J. T.: The ToF-ACSM: a portable
633 aerosol chemical speciation monitor with TOFMS detection, *Atmos. Meas. Tech.*, 6, 3225–3241,
634 <https://doi.org/10.5194/amt-6-3225-2013>, 2013.
- 635 Guieu, C., D'Ortenzio, F., Dulac, F., Taillandier, V., Doglioli, A., Petrenko, A., Barrillon, S., Mallet, M., Nabat,
636 P., and Desboeufs, K.: Process studies at the air-sea interface after atmospheric deposition in the
637 Mediterranean Sea: objectives and strategy of the PEACETIME oceanographic campaign (May–June
638 2017), *Biogeosciences Discuss.*, <https://doi.org/10.5194/bg-2020-44>, in review, 2020.
- 639 Giordano, M. R., Kalnajs, L. E., Avery, A., Goetz, J. D., Davis, S. M., and DeCarlo, P. F.: A missing source of
640 aerosols in Antarctica – beyond long-range transport, phytoplankton, and photochemistry, *Atmos.*
641 *Chem. Phys.*, 17, 1–20, <https://doi.org/10.5194/acp-17-1-2017>, 2017.
- 642 Harvey, G. Microlayer collection from the sea surface: a new method and initial results. *Limnol. Oceanogr.* 11, 608–
643 613. doi: 10.4319/lo.1966.11.4.0608, 1966
- 644 Kuznetsova, M., Lee, C., Aller, J. Characterization of the proteinaceous matter in marine aerosols. *Mar. Chem.*
645 96, 359–377. <https://doi.org/10.1016/j.marchem.2005.03.007>, 2005
- 646 Leroux, R., G. Grégori, K. Leblanc, F. Carlotti, M. Thyssen, M. Dugenne, M. Pujó-Pay, P. Conan, M.-P.
647 Jouandet, N. Bhairy, L. Berline Combining laser diffraction, flow cytometry and optical microscopy to
648 characterize a nanophytoplankton bloom in the northwestern Mediterranean. *Prog Oceanogr.* 163, 248–
649 259. <https://doi.org/10.1016/j.pocean.2017.10.010>, 2017.
- 650 McCluskey, C.S., Hill, T.C., Malfatti, F., Sultana, C.M., Lee, C., Santander, M.V., Beall, C.M., Moore, K.A.,
651 Cornwell, G.C., Collins, D.B.. A dynamic link between ice nucleating particles released in nascent sea
652 spray aerosol and oceanic biological activity during two mesocosm experiments. *J. Atmospheric Sci.*
653 74, 151–166. <https://doi.org/10.1175/JAS-D-16-0087.1>, 2017.
- 654 MerMex Group, Marine ecosystems' responses to climatic and anthropogenic forcings in the Mediterranean,
655 *Prog Oceanogr* doi:10.1016/j.pocean.2011.02.003, 91 (2011) 97–166
656 <https://doi.org/10.1016/j.pocean.2011.02.003>, 2011.
- 657 Middlebrook, A.M., Bahreini, R., Jimenez, J.L., Canagaratna, M.R. Evaluation of composition-dependent
658 collection efficiencies for the aerodyne aerosol mass spectrometer using field data. *Aerosol Sci.*
659 *Technol.* 46, 258–271. <https://doi.org/10.1080/02786826.2011.620041>, 2012.
- 660 O'Dowd, C.D., Facchini, M.C., Cavalli, F., Ceburnis, D., Mircea, M., Decesari, S., Fuzzi, S., Yoon, Y.J., Putaud,
661 J.-P. Biogenically driven organic contribution to marine aerosol. *Nature* 431, 676.
662 DOI:10.1038/nature02959, 2004.



- 663 O'Dowd, C., Ceburnis, D., Ovadnevaite, J. *et al.* Connecting marine productivity to sea-spray *via* nanoscale
664 biological processes: Phytoplankton Dance or Death Disco?. *Sci Rep* 5, 14883.
665 <https://doi.org/10.1038/srep14883>, 2015.
- 666 Ovadnevaite, J., O'Dowd, C., Dall'Osto, M., Ceburnis, D., Worsnop, D.R., Berresheim, H. Detecting high
667 contributions of primary organic matter to marine aerosol: A case study. *Geophys. Res. Lett.* 38.
668 DOI: 10.1029/2010GL046083, 2011
- 669 Rinaldi, M. *et al.* Chemical characterization and source apportionment of size-segregated aerosol collected at an
670 urban site in Sicily. *Water Air Soil Poll* 185, 311–21, doi:10.1007/s11270-007-9455-4, 2007.
- 671 Rinaldi, M., Fuzzi, S., Decesari, S., Marullo, S., Santolero, R., Provenzale, A., Von Hardenberg, J., Ceburnis, D.,
672 Vaishya, A., O'Dowd, C.D. Is chlorophyll-a the best surrogate for organic matter enrichment in
673 submicron primary marine aerosol? *J. Geophys. Res. Atmos* 118, 4964–4973.
674 <https://doi.org/10.1002/jgrd.50417>, 2013.
- 675 Sandrini, S. *et al.* Size-resolved aerosol composition at an urban and a rural site in the Po Valley in summertime:
676 implications for secondary aerosol formation. *Atmos. Chem. Phys.* 16, 10879–10897, doi:10.5194/acp-
677 16-10879-2016, 2016.
- 678 Schmale, J., Schneider, J., Nemitz, E., Tang, Y. S., Dragosits, U., Blackall, T. D., Trathan, P. N., Phillips, G. J.,
679 Sutton, M., and Braban, C. F.: Sub-Antarctic marine aerosol: dominant contributions from biogenic
680 sources, *Atmos. Chem. Phys.*, 13, 8669–8694, <https://doi.org/10.5194/acp-13-8669-2013>, 2013.
- 681 Schneider, J., Freutel, F., Zorn, S. R., Chen, Q., Farmer, D. K., Jimenez, J. L., Martin, S. T., Artaxo, P.,
682 Wiedensohler, A., and Borrmann, S.: Mass-spectrometric identification of primary biological particle
683 markers and application to pristine submicron aerosol measurements in Amazonia, *Atmos. Chem.*
684 *Phys.*, 11, 11415–11429, <https://doi.org/10.5194/acp-11-11415-2011>. 2011.
- 685 Schwier, A. N., Rose, C., Asmi, E., Ebling, A. M., Landing, W. M., Marro, S., Pedrotti, M.-L., Sallon, A.,
686 Iuculano, F., Agustí, S., Tsiola, A., Pitta, P., Louis, J., Guieu, C., Gazeau, F., and Sellegri, K.: Primary
687 marine aerosol emissions from the Mediterranean Sea during pre-bloom and oligotrophic conditions:
688 correlations to seawater chlorophyll *a* from a mesocosm study, *Atmos. Chem. Phys.*, 15, 7961–7976,
689 <https://doi.org/10.5194/acp-15-7961-2015>, 2015.
- 690 Seinfeld and Pandis, *Atmospheric Chemistry and Physics: From Air Pollution to Climate Change*, Third edition,
691 Hoboken, New Jersey : John Wiley & Sons, Inc., [2016] ©2016
- 692 Sellegri K., Nicosia, A., Freney, E., Uitz, J., Thyssen, M., Grégori, G., Engel, A., Zäncker, B., Haëntjens, N.,
693 Mas, S., Picard, D., Saint-Macary, A., Peltola, M., Rose, C., Trueblood, J.T., Lefevre, D., D'Anna, B.,
694 Desboeuf, K., Meskhidze, N., Guieu, C and Law, C. S., Surface ocean microbiota determine cloud
695 precursors, submitted
- 696 Slade, W.H, Boss, E., Dall'Olmo, G., Langner, M.R., Loftin, J., Behrenfeld, M.J. and Roesler, C., Underway and
697 moored methods for improving accuracy in measurement of spectral particulate absorption and



- 698 attenuation. J Atmos Ocean Tech, 27:10, 1733-1746.
699 <https://doi.org/10.1175/2010JTECHO755.1>, 2010
- 700 Tobler, A. K, Skiba, A, Wang, D.S, Croteau, P, Styszko, K, Nęcki, J, Baltensperger, U, Slowik, J.G., and
701 Prévôt A.S. H. Improved chloride quantification in quadrupole aerosol chemical speciation monitors
702 (Q-ACSMs), submitted to Atmos. Meas Tech.
- 703 Thyssen, M., G. Grégori, J -M Grisoni, M. Pedrotti, L. Mousseau, L.F. Artigas, S. Marro, N. Garcia, O.
704 Passafiume and M.J. Denis, Onset of the spring bloom in the northwestern Mediterranean Sea :
705 influence of environmental pulse events on the in situ hourly-scale dynamics of the phytoplankton
706 community structure. *Front. Microbiol.* 5:387. doi:10.3389/fmicb.2014.003872014, 2010.
- 707 Timonen, H., Cubison, M., Aurela, M., Brus, D., Lihavainen, H., Hillamo, R., Canagaratna, M., Nekat, B.,
708 Weller, R., Worsnop, D., and Saarikoski, S.: Applications and limitations of constrained high-resolution
709 peak fitting on low resolving power mass spectra from the ToF-ACSM, Atmos. Meas. Tech., 9, 3263–
710 3281, <https://doi.org/10.5194/amt-9-3263-2016>, 2016.
- 711 Trueblood, J. T, Nicosia A., Engel, A, Zäncker, B., Rinaldi M., Freney E, Thyssen, M, Obernosterer I,
712 Dinasquet, J, Haëntjens, N, Belosi, F, Santachiara, G, Guieu, C, and Sellegri, K: A Two-Component
713 Parameterization of Marine Ice Nucleating Particles Based on Seawater Biology and Sea Spray Aerosol
714 Measurements During the PEACETIME Cruise in the Mediterranean Sea, in prep, 2020
- 715 Vlachou, A., Tobler, A., Lamkaddam, H., Canonaco, F., Daellenbach, K. R., Jaffrezo, J.-L., Minguillón, M. C.,
716 Maasikmets, M., Teinemaa, E., Baltensperger, U., El Haddad, I., and Prévôt, A. S. H.: Development of
717 a versatile source apportionment analysis based on positive matrix factorization: a case study of the
718 seasonal variation of organic aerosol sources in Estonia, Atmos. Chem. Phys., 19, 7279–7295,
719 <https://doi.org/10.5194/acp-19-7279-2019>, 2019.
- 720 Wang, X., Sultana, C.M., Trueblood, J., Hill, T.C., Malfatti, F., Lee, C., Laskina, O., Moore, K.A., Beall, C.M.,
721 McCluskey, C.S. Microbial control of sea spray aerosol composition: a tale of two blooms. *ACS Cent.*
722 *Sci.* 1, 124–131. <https://doi.org/10.1021/acscentsci.5b00148>, 2015.
- 723 Yoon, Y., Ceburnis, D., Cavalli, F., Jourdan, O., Putaud, J., Facchini, M., Decesari, S., Fuzzi, S., Sellegri, K.,
724 Jennings, S. Seasonal characteristics of the physicochemical properties of North Atlantic marine
725 atmospheric aerosols. *J. Geophys. Res. Atmos* 112.
726 <https://doi.org/10.1029/2005JD007044>, 2007
727
728